

See discussions, stats, and author profiles for this publication at: <https://www.researchgate.net/publication/51867209>

Stop Signals Provide Cross Inhibition in Collective Decision-Making by Honeybee Swarms

Article in Science · December 2011

DOI: 10.1126/science.1210361 · Source: PubMed

CITATIONS

218

READS

442

6 authors, including:



Thomas Seeley

Cornell University

180 PUBLICATIONS 12,441 CITATIONS

[SEE PROFILE](#)



Nigel R Franks

University of Bristol

316 PUBLICATIONS 19,183 CITATIONS

[SEE PROFILE](#)



James A R Marshall

The University of Sheffield

142 PUBLICATIONS 2,329 CITATIONS

[SEE PROFILE](#)

Some of the authors of this publication are also working on these related projects:



Brains on Board [View project](#)



Honey bees in the wild [View project](#)



Supporting Online Material for

Stop Signals Provide Cross Inhibition in Collective Decision-Making by Honeybee Swarms

Thomas D. Seeley,* P. Kirk Visscher, Thomas Schlegel, Patrick M. Hogan, Nigel R. Franks, James A. R. Marshall

*To whom correspondence should be addressed. E-mail: tds5@cornell.edu

Published 8 December 2011 on *Science Express*
DOI: 10.1126/science.1210361

This PDF file includes:

Materials and Methods
SOM Text
Figs. S1 to S4
Tables S1 and S2
References

Other Supporting Online Material for this manuscript includes the following:
available at www.sciencemag.org/cgi/content/full/science.1210361/DC1

Movie S1

Materials and Methods

Study Sites and Bees

The initial observations of stop signaling were made at the Liddell Field Station of Cornell University, in Ithaca, NY (42°26'N, 76°30'W) using a natural swarm. On 12 Aug 2009, a swarm emerged from a hive and the next morning we made video and sound recordings of 20 nest-site scouts performing waggle dances on this swarm. On 2 June 2011, we captured a second swarm and the following day we made recordings of another 20 nest-site scouts as they performed waggle dances on their swarm. Additional observational work, to determine when in the course of performing a waggle dance a scout receives stop signals, was conducted using three artificial swarms in June and early July 2010 at the Liddell Field Station. All of the experimental work was conducted in late July 2010 using artificial swarms at the Shoals Marine Laboratory on Appledore Island, Maine (42°58'N, 70°37'W). This 39-ha island is nearly treeless and so has few natural nest cavities for honey bees. Here we could set out nest boxes and be confident that they would receive attention from the scouts of the swarms that we prepared from colonies brought to the island. All of the honey bees (*Apis mellifera*) used in this study came from colonies headed by open-mated queens of Italian stock purchased from a queen breeder (C. F. Koehnen and Sons, Glenn, CA).

Preparing Artificial Swarms

We simulated the process of swarming by feral colonies, a sequence of events that includes several thousand worker bees: (i) leaving the parental hive with their mother queen and with a food reserve sequestered in their bodies (25, 26), (ii) clustering together for a few days while scout bees find prospective nest sites and choose the best one (21, 27), and (iii) flying en masse to the chosen dwelling place (28). Therefore, to prepare a swarm, we took from a colony its queen and 0.8 kg of workers (~6,200 bees) (29) and placed them in a wooden box (15x25x35 cm) that was screened on its two largest sides for ventilation (19). The queen was placed in a small (1.6x3.2x10 cm) screened cage that was suspended from the lid of the box so that the workers could cluster around her. This

“package” of bees was placed in a shaded location and for the next three days the bees were fed a sucrose solution (1:1 vol:vol, sucrose and water) ad libitum by repeatedly brushing the solution on one of the screened sides of the box where the workers could drink it. By the end of the three days, the workers had distended abdomens and were secreting copious wax scales, traits that are characteristic of workers in real swarms. The swarm was then transferred to a swarm stand, which consisted of a post supporting a flat vertical board (40x40 cm) with an opening to hold the queen cage (27). The worker bees formed a compact cluster over the queen cage on one side of the swarm stand. With the swarm so arranged, it was easy to monitor the waggle dances performed by nest-site scouts on the surface of the swarm cluster. The clustering and dancing behaviors of the bees did not differ between our natural and artificial swarms. Indeed, many studies with artificial swarms, spanning more than half a century, have uncovered no differences in behavior from natural swarms (12).

Apparatus

To determine when waggle dancers received stop signals or produced piping signals, a small electric condenser microphone (Radio Shack Model 33-3013, 70-16,000 Hz frequency response) was plugged into a video camera (Sony DCR-TRV50) and its output was monitored through headphones. A 40 mm length of 8 mm internal diameter Tygon tubing was attached to the microphone to make it directional. The microphone was held 1-2 cm from dancing bees on the swarm cluster’s surface to record when the dancers received stop signals and when other bees nearby produced piping signals.

The two nest boxes that provided potential home sites on Appledore Island were the same as those used in previous studies (6, 30). The cavity volume and entrance size of each nest box was adjustable, but we left these properties set at 40 l and 15 cm², so that both nest boxes provided a highly desirable nest cavity. Each box was housed in a separate, open-sided shelter (30) so that they had identical exposures to wind, sun, and rain.

Video Recording and Transcription for Observational Studies

Nest-site scouts performing waggle dances on the surface of each swarm were video recorded and tracked with the microphone as described above. Each dancing bee was followed from shortly after she started dancing to until she stopped dancing. The video recordings made in August 2009 and June 2011 were played back in slow motion with a video deck (Sony DSR-30). We noted the start and stop times (with 1/30th s precision) of each waggle run and each stop signal, and the location on the dancer's body where each stop signal was received. The video recordings made in June and early July 2010 were played back at normal speed. For each dance, we counted the number of dance circuits performed, the number of stop signals received, and when in the dance (during which circuit) each stop signal was received.

Layout for Experimental Studies

For the first two trials of the experimental work, the layout consisted of a swarm positioned in the center of Appledore Island and two nest boxes placed 250 m away on the eastern side of the island, 40 m apart (the locations designated as sites 3 and 4 in Fig. 2 in 30). For two later trials of the experiment, the layout was the same except that only one nest box was provided.

Scout Marking for Experiments

Once the swarm bees had clustered around the caged queen on the swarm stand, an observer was stationed at each nest box to record when it was discovered by a scout bee and to label the scout bees visiting it. When a scout arrived, she was caught in a 15-cm diameter, 40-cm deep insect net, by placing it over the nest box entrance while the bee was inside. The trapped bee was marked gently with a spot of paint (Sharpie oil-based paint marker) on her thorax and then released. The time at which each scout was marked was recorded. The scouts at one nest box received yellow paint marks and those at the other nest box received pink paint marks.

Video and Sound Recording for Experiments

Meanwhile, at the swarm, a third observer observed and video recorded the activities of bees on the surface of the swarm throughout the process of choosing a nest site and of

implementing the decision. If an unmarked bee performed a waggle dance, she was removed from the swarm to prevent buildup of scouting of unmonitored sites. When a marked bee danced, the video camera was turned on and the microphone was held within 2 cm of her to know when she received a stop signal, which could be heard through the headphones. When the dancer being monitored received a stop signal, the observer identified which bee sent the signal by noticing which individual lunged toward her (13). The observer announced whether the sender was carrying either a pink or yellow paint mark, for later transcription from the videotape audio track. Sometimes the bee that sent a particular stop signal could not be identified immediately, but in most such cases the sender could be identified when we replayed the video recording in slow motion and noticed which bee pressed against the dancer at the moment the stop signal was produced. For a small minority (~2%) of the stop signals, we could not identify the sender; usually these were signals produced when the microphone obscured the dancer.

Video Transcription for Experiments

We played back the video recordings of each swarm and noted each instance of observing a marked bee performing a waggle dance, the time during which this occurred, the number of dance circuits the dancer produced, the color of the dancer's paint mark, and the color of the paint mark of each bee (if any) that directed a stop signal at the dancer. We also played back the video recordings a second time to count the number of worker piping signals audible in the background within each 5-min period. Once a quorum of scout bees is reached at the chosen site, scouts from this site begin to produce piping signals at the swarm cluster to stimulate the other bees in the cluster to warm up their flight muscles in preparation for takeoff (19, 31). Thus, the onset of worker piping marks the transition from decision making to decision implementation in a swarm of bees. We defined the time of this transition for each swarm as the starting edge of the first series of three 5-minute intervals in which we heard worker piping in each of the three intervals.

Statistical Analyses

To analyze the distribution of stop signals during waggle dances, we divided each dance into tenths (based on the number of circuits in the dance), and each stop signal was

scored with respect to the decile of the dance in which the signal was received. If stop signals were equally likely to occur at any point during the dance, the expected value overall for each dance decile would equal $1/10^{\text{th}}$ of the observed stop signals.

Significance of the departure from this expected distribution was evaluated with a Chi-squared goodness-of-fit test.

To test for biases in the delivery of signals by scouts, we compared the observed signals to the proportions expected if scouts from either site were equally likely to perform "ipsi" signals (i.e., signals on dancers for same site) and "contra" signals (i.e., signals on dancers for the other site). Dancers that receive stop signals usually receive them from more than one scout, but often a single signaler delivers more than one stop signal to the same dancer (Fig. S1). Therefore, we performed this analysis in two ways, one that overstates and one that understates the likelihood of the observed result under the null hypothesis.

The first, more conservative approach, made the assumption that all signals to a given dancer by a scout with a particular color mark were made by the same scout, so each dance was scored as having a minimum of zero or one contra-signalers and zero or one ipsi-signalers (thus zero to two minimum total signalers per dance). These signaler minima were summed over both 2-site trials, separately for the decision and implementation phases. We calculated the corresponding expected sums of ipsi-signaler minima over all dances of the decision phase (from first dance to start of piping) under the null hypothesis of no bias, as follows

$$Exp_{Ipsi} = \sum_{d=FirstDance_{phase}}^{LastDance_{phase}} \frac{IpsiScouts_d}{IpsiScouts_d + ContraScouts_d} MinTotalSignalers_d$$

using the number of scouts that had been marked at each of the two sites at the time each dance was observed, and the minimum number of signalers that could have delivered the stop signals observed for that dance. Exp_{Contra} was calculated in a parallel manner, as were the expectations for both types of signals during the implementation phase (from

start of piping to last dance). Then, separately for the decision and implementation phases, we performed Chi-squared goodness-of-fit tests between the sums of each type of signal and the corresponding expected values. To the extent that there were actually more scouts than the minimum assumed performing stop signals on a given dance, this approach lumps independent signalers together, reduces the power of the statistical test, and so overstates the likelihood of the result under the null hypothesis.

In a less conservative approach, we performed a similar analysis of the observed number of ipsi and contra stop signals for each dance, and calculated the expected values with the same formula, but with StopSignals_d in place of $\text{MinTotalSignalers}_d$. To the extent that single scouts perform multiple signals on the same dance, this approach splits non-independent signals as if they were independent and so understates the likelihood of the result under the null hypothesis. The two approaches thus bracket the true likelihood.

To test for differences in the incidence of stop signaling, we summed the counts of dances that received stop signals (even if these were by unmarked or unidentified bees), or that did not receive stop signals, over all 4 trials, in a 2x2x2 table with signaled/unsignaled, 1-site/2-site, and decision-phase/implementation-phase axes. This table was then split and separately analyzed in the decision and implementation phases for homogeneity between the 1-site and 2-site trials in the proportion of dances that received stop signals, using a Chi-squared test of homogeneity.

SOM Text

Models of Decision Making

Current models of decision making in nervous systems and insect societies (3, 8, 10), which feature competition between mutually interacting populations of excitable units,

work well when the alternatives are very different. In the case of equal alternatives studied here, however, they often break down: these models can become deadlocked, with equal numbers of individual units committed to either alternative, and will therefore be unable to make a decision without further external input. Drift-diffusion models eventually escape deadlock due to noise (32), but spend an extremely long time accumulating enough evidence to choose between identical alternatives, an unnecessary delay. Solutions to this problem from psychology and neuroscience include assuming that subjects learn thresholds appropriate to the common signal levels (zero when there is no signal to integrate) (10), and time-dependent reduction of decision thresholds or increase in gain (33).

We begin by demonstrating the problem of decision making over equal alternatives in the direct-switching model of 3. We model the decision-making process of mutually interacting populations of excitable units (for example, individual neurons or bees) with an analytical, individual-level stochastic model of opinion formation (34-36). In this bottom-up approach, we begin with a stochastic description of the entire system at the individual level, from which we derive analytically the emergent, average (mean-field) population-level behavior of the whole system. This provides a rigorous means of deriving the population-level equations that would normally be postulated by a modeler (as in 3, for example). Crucially, in this case, the derived population-level equations agree with those that would be chosen by a modeler.

Microscopic, Individual-level Model

For a binary-choice decision-making process between two competing alternatives, we consider each individual unit as belonging to one of three populations: either uncommitted to either alternative, labelled U ; committed to alternative A ; or committed to alternative B . Each individual may stochastically interact in a number of different ways with each of the other individual units, with each possible interaction having a particular probability per unit time; this describes a continuous-time Markov process. For the direct-switching model of Fig. 4 in 3, the possible interactions between individual units are:

Commitment — an uncommitted unit U may spontaneously commit to either alternative A or B (e.g., through the discovery of a nest site in the case of nest-site selection in honey bee swarms, or the input signal from the medial temporal neurons (37) integrated by the lateral intraparietal neurons (38, 39) in the case of a perceptual binary-choice task in primate brains) with probabilities per unit time γ_A and γ_B respectively:



Abandonment/decay — a unit committed to either alternative may spontaneously abandon its commitment and revert to an uncommitted state (e.g., through loss of interest in a nest site in the case of honey bees, or leakage from the lateral intraparietal neurons in the case of primate brains):



Recruitment — a unit committed to either alternative may actively recruit an uncommitted unit, convincing the latter to commit to the alternative favored by the former (e.g., through the waggle dance in the case of honey bees, tandem running in the case of ants, or synaptic connections in the case of primate brains):



Direct switching — a unit committed to either alternative may actively switch the commitment of another unit already committed to the other alternative, convincing the latter to commit to the alternative favored by the former (through mechanisms similar or identical to those used for recruitment):



The total number of individual units $N = N_A + N_B + N_U$ is fixed, leaving only two independent variables N_A and N_B , and all rates $\{\gamma_i, \alpha_i, \rho_i, \delta_i\}$ are strictly greater than zero. For this continuous-time Markov process, we may then write down a microscopic, continuous-time master equation for the system from the individual-level interactions in the standard manner (40). This differential equation describes every possible state $\{N_A, N_B, N_U\}$ that the system can occupy at the individual level and, by taking into account all of the possible interactions between all possible combinations of individuals, how the probability of being in each of these states $P(N_A, N_B, t)$ evolves as a function of time t .

Emergent Macroscopic, Population-level Model

Provided that the total number of decision-making units (insect scouts or neurons in the lateral intraparietal area [41-43]) is not too small (as is the case for the honey bee swarms studied in the main text), we may use a van Kampen expansion (40) to derive analytically the emergent, average (mean-field) population-level behavior from the master equation (see, for example, the system described in 44). The leading-order $N^{1/2}$ term in the van Kampen expansion results in two coupled mean-field, population-level equations describing the dynamics of the proportions $\Psi_i = N_i/N$ of individual units committed to either alternative:

$$\begin{aligned}\frac{d\Psi_A}{dt} &= \gamma_A(1 - \Psi_A - \Psi_B) - \Psi_A[\alpha_A - \rho_A(1 - \Psi_A - \Psi_B) + (\delta_B - \delta_A)\Psi_B] \\ \frac{d\Psi_B}{dt} &= \gamma_B(1 - \Psi_A - \Psi_B) - \Psi_B[\alpha_B - \rho_B(1 - \Psi_A - \Psi_B) + (\delta_A - \delta_B)\Psi_A].\end{aligned}$$

These deterministic equations describe the mean-field, macroscopic behavior of the direct-switching decision-making process proposed in 3, and are the noise-free equivalents of Equation (6.4) in that reference. Note, therefore, that the derived population-level equations agree with those chosen based on a systems-level description of the model (3).

For the case that the decay rates $\alpha_i = 0$, the noisy equivalent of this direct-switching decision-making process asymptotically converges to a drift-diffusion process along the line $\Psi_A + \Psi_B = 1$ (3). By inspection of Equation (6.5) in 3, we see that in this asymptotic case with unequal alternatives, there will always be two fixed points, $\Psi^1 = (0,1)$ and $\Psi^2 = (1,0)$; the fixed point corresponding to the superior alternative will always be stable, the other always unstable.

This one-dimensional decision-making process along the line is exactly equivalent to the decision-making strategy which statistically optimizes the trade-off between speed and accuracy when deciding between two alternatives with uncertain information. The direct-

switching decision-making process is therefore described as “asymptotically optimal” (3). The fixed-points and the dynamical behavior of this system are illustrated in Fig. S1A.

The Problem of Deadlock for Equal Alternatives

This statistically optimal decision-making process becomes problematic when the alternatives are equal. In this case, the two fixed-points from the unequal case disappear, and are replaced by one physical, stable attractor, the one-dimensional manifold $\Psi_A + \Psi_B = 1$. This is illustrated in Fig. S1B. Upon reaching this manifold, there is no further deterministic dynamical motion: there is zero drift, and it will take a very long time to stochastically accumulate enough information for diffusion alone to allow the system to pass a decision threshold, unless the thresholds can be set appropriately to zero, or reduced over time. In some biological systems, such as house-hunting insects, decisions can be rare and unpredictable life-events, precluding the *a priori* selection of the best threshold for a given instance of a decision problem, as *can* be done for subjects in controlled experimental regimes (10). Similarly, while time-dependent recovery from “stalled” decision-making processes, such as those with zero drift, can be achieved (33), the time and hence the fitness cost could be prohibitive, such as the reduced survival probability of an emigrating social insect colony. A decision between equal alternatives should be made quickly as there is no difference between them, whereas a decision between unequal alternatives should be slower, to ascertain which is superior. For a real biological system, which should not be indecisive when it does not matter which alternative is chosen, a better behavior in the case of equal alternatives would be to randomly choose either alternative as quickly as possible; drift-diffusion decision making does not automatically have this property.

Of even more concern is the dynamical behavior of the direct-switching model for equal alternatives when the asymptotic assumption of zero decay is relaxed. In any real biological system natural decay will be inevitable, as not all committed individuals will be able to retain their commitments indefinitely for any number of different reasons (e.g,

death, forgetfulness, neuronal leakage, etc.). In this case, the stable one-dimensional manifold vanishes, and is replaced with a stable, attractive fixed-point:

$$\Psi_A^s = \Psi_B^s = \frac{\rho - \alpha - 2\gamma + \sqrt{(\rho - \alpha - 2\gamma)^2 + 8\gamma\rho}}{4\rho}.$$

Making the rotation (10)

$$\begin{pmatrix} x_1 \\ x_2 \end{pmatrix} = \frac{1}{\sqrt{2}} \begin{pmatrix} 1 & -1 \\ 1 & 1 \end{pmatrix} \cdot \begin{pmatrix} \Psi_A \\ \Psi_B \end{pmatrix},$$

we may perform a linear stability analysis about the physical fixed-point $\Psi^s \rightarrow \mathbf{x}^s$. It can be shown (using symbolic algebra software or otherwise) that the eigenvalues of the corresponding stability matrix are strictly negative and distinct, and hence that this fixed-point is a stable attractor for all parameters values $\{\gamma, \alpha, \rho, \delta\}$ in the symmetric case. This is illustrated in Fig. S1C.

Hence, for even infinitesimally small amounts of decay, this decision-making process becomes deadlocked at indecision, with equal numbers of individual units committed to either alternative. This problem of deadlock in the direct-switching model, and other models, is clearly pathological for a real biological system.

Indiscriminate Stop-signal Model

We now investigate the population-level behavior conferred by the stop signal found in honey bees. This individual-level interaction involves bees committed to a given alternative inhibiting the commitment of other bees, rather than switching them. The stop signal could be either indiscriminately directed at any other committed individuals, or discriminately directed only at individuals committed to the other alternative. In this section, we show that the indiscriminately directed stop signal shows no qualitative change in the population-level behavior of the system, which still becomes deadlocked when the alternatives are equal.

For the indiscriminate stop-signal model, the possible interactions between individual units are:

Commitment — an uncommitted unit may spontaneously commit to either alternative:



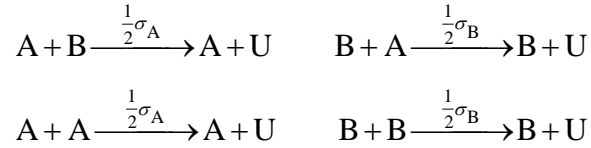
Abandonment/decay — a unit committed to either alternative may spontaneously abandon its commitment and revert to an uncommitted state:



Recruitment — a unit committed to either alternative may actively recruit an uncommitted unit, convincing the latter to commit to the alternative favored by the former:



Indiscriminate stop signal — a unit committed to either alternative may actively inhibit the commitment of a unit already committed to either alternative, convincing the latter to lose their commitment and become uncommitted:



Writing down the corresponding microscopic master equation and performing a van Kampen expansion yields the following mean-field, population-level equations:

$$\begin{aligned} \frac{d\Psi_A}{dt} &= \gamma_A(1 - \Psi_A - \Psi_B) - \Psi_A[\alpha_A - \rho_A(1 - \Psi_A - \Psi_B) + \frac{1}{2}(\sigma_A\Psi_A + \sigma_B\Psi_B)] \\ \frac{d\Psi_B}{dt} &= \gamma_B(1 - \Psi_A - \Psi_B) - \Psi_B[\alpha_B - \rho_B(1 - \Psi_A - \Psi_B) + \frac{1}{2}(\sigma_A\Psi_A + \sigma_B\Psi_B)] , \end{aligned}$$

where all rates $\{\gamma_i, \alpha_i, \rho_i, \sigma_i\} > 0$.

In the case of equal alternatives, there again exists only one physical fixed-point Ψ^s , with equal numbers of individual units committed to either alternative:

$$\Psi_A^s = \Psi_B^s = \frac{\rho - \alpha - 2\gamma + \sqrt{(\rho - \alpha - 2\gamma)^2 + 4\gamma(2\rho + \sigma)}}{2(2\rho + \sigma)} .$$

Rotating into the (x_1, x_2) coordinate system and performing a linear stability analysis about the physical fixed-point $\Psi^s \rightarrow \mathbf{x}^s$, we find that the eigenvalues of the corresponding stability matrix are again strictly negative and distinct, and hence that this fixed-point is

also a stable attractor for all parameters values $\{\gamma, \alpha, \rho, \sigma\}$ in the symmetric case. This is illustrated in Fig. S2.

The indiscriminately-directed stop-signal model therefore shows no qualitative change in the population-level behavior of the system for equal alternatives compared to other deadlocked models such as the direct-switching model. This decision-making process also becomes deadlocked at indecision, with equal numbers of individual units committed to either alternative.

Discriminate Stop-signal Model

In this section, we show that the discriminately-directed stop signal causes a significant qualitative change in the population-level behavior of the system, greatly improving the reliability of honey bee collective decision making by enabling the bees to overcome the problem of indecision and deadlock when the alternatives are equal.

For the discriminate stop-signal model, the possible interactions between individual units are the same as for the indiscriminate stop-signal model, with one modification so that the stop signal is now directed only at individuals committed to the other alternative:

Discriminate stop signal — a unit committed to one alternative may only actively inhibit the commitment of a unit already committed to the *other* alternative, convincing the latter to lose its commitment and become uncommitted:



Writing down the corresponding microscopic master equation and performing a van Kampen expansion yields the following mean-field, population-level equations:

$$\begin{aligned} \frac{d\Psi_A}{dt} &= \gamma_A(1 - \Psi_A - \Psi_B) - \Psi_A[\alpha_A - \rho_A(1 - \Psi_A - \Psi_B) + \sigma_B\Psi_B] \\ \frac{d\Psi_B}{dt} &= \gamma_B(1 - \Psi_A - \Psi_B) - \Psi_B[\alpha_B - \rho_B(1 - \Psi_A - \Psi_B) + \sigma_A\Psi_A], \end{aligned}$$

where all rates $\{\gamma_i, \alpha_i, \rho_i, \sigma_i\} > 0$. Again, note that these derived equations agree with those a modeler would be expected to choose as a top-down description of the system. In

this case, there is a qualitative change in the behavior of the decision-making system, for both equal and unequal alternatives.

Equal Alternatives. In this case, there is a bifurcation as an increasing function of the size of the stop signal. Below the critical size σ^* of the stop signal, there exists the same physical fixed-point \mathbf{x}^s as for the indiscriminate stop-signal model, with equal numbers of individual units committed to either alternative:

$$x_1^s = 0 \quad \text{and} \quad x_2^s = \frac{\rho - \alpha - 2\gamma + \sqrt{(\rho - \alpha - 2\gamma)^2 + 4\gamma(2\rho + \sigma)}}{\sqrt{2}(2\rho + \sigma)} .$$

Again performing a linear stability analysis about the physical fixed-point \mathbf{x}^s , we find that the eigenvalues of the corresponding stability matrix are again strictly negative (provided $\sigma < \sigma^*$) and distinct, and hence that prior to the bifurcation this fixed-point is again a stable attractor for all parameters values $\{\gamma, \alpha, \rho, \sigma < \sigma^*\}$ in the symmetric case. This is illustrated in Fig. S3A.

As the size of the stop signal is increased, and provided that $\rho > \alpha$, the stable fixed-point \mathbf{x}^s bifurcates at the critical value

$$\sigma^* = \frac{4\alpha\gamma\rho}{(\rho - \alpha)^2} .$$

At this critical value of stop signal size, one of the eigenvalues of the linearised stability matrix about \mathbf{x}^s changes sign, becoming strictly positive with the other remaining strictly negative. Hence after the bifurcation this fixed-point changes to an unstable saddle point for all parameters values $\{\gamma, \alpha, \rho > \alpha, \sigma > \sigma^*\}$ in the case of equal alternatives.

The condition for the bifurcation ($\rho > \alpha$) is rather intuitive and is not a stringent condition biologically: individual units need to be recruited quicker (as described by ρ) than they abandon their commitment (as described by α). Otherwise, if $\rho < \alpha$, the decision-making populations will not be able to grow sufficiently to reach a decision-making threshold.

In addition, two further physical fixed-points \mathbf{x}^\pm appear after the bifurcation:

$$x_1^\pm = \pm \frac{\sqrt{(\rho - \alpha)^2 - 4\alpha\gamma\rho/\sigma}}{\rho\sqrt{2}} \quad \text{and} \quad x_2^\pm = \frac{\rho - \alpha}{\rho\sqrt{2}}.$$

Similarly, it may be shown that the eigenvalues of the stability matrix for both fixed-points \mathbf{x}^\pm are strictly negative and in both cases distinct, and hence that both of these fixed-points are stable attractors for all parameters values $\{\gamma, \alpha, \rho > \alpha, \sigma > \sigma^*\}$ in the symmetric case. The three fixed-points which appear after the bifurcation are illustrated in Fig. S3B.

The discriminate stop-signal model therefore shows a significant qualitative change in the population-level behavior of the system, greatly improving the reliability of collective decision making by honey bee swarms by enabling them to overcome the problem of indecision and deadlock when the alternatives are equal. They will choose either alternative randomly, but will do so quickly and decisively.

Furthermore, we have shown that to achieve this prompt decision making, the stop signal must be discriminate (targeted), as reported empirically in the main text. If it is untargeted, the stop signal will result in indecision and deadlock; it is specifically *cross* inhibition which solves the problem of deadlock and increases the reliability of the bees' collective decision making.

Unequal Alternatives. Other models of decision making work well when the alternatives are very different. In such asymmetric cases, the discriminate stop-signal model adapts its behavior as the magnitude of the difference in any of the parameters of the model ($\Delta\gamma = \gamma_A - \gamma_B$, $\Delta\alpha = \alpha_A - \alpha_B$, $\Delta\rho = \rho_A - \rho_B$, $\Delta\sigma = \sigma_A - \sigma_B$) increases; in such cases, the discriminate stop-signal model is thereby also expected to converge on choosing the superior alternative.

The analytical details in this asymmetric case are somewhat involved, and will be presented and explored more thoroughly in future work since it is not studied empirically presently. However, numerical investigations show that starting with the symmetrical

equal-alternatives case after the stop-signal bifurcation (Fig. S3B), as the magnitude of the difference in any of the parameters of the model is increased, the initial, symmetrically located unstable fixed-point moves towards the part of the phase plane corresponding to the inferior alternative. At a critical value of $|\Delta\gamma|^*$, $|\Delta\alpha|^*$, $|\Delta\rho|^*$ or $|\Delta\sigma|^*$ this unstable fixed-point coalesces with the stable fixed-point corresponding to the inferior alternative. Above these critical parameter values, the system has again only one asymmetrically located stable fixed-point corresponding to the superior alternative, and will therefore then be expected to converge on choosing that superior alternative, as illustrated in Fig. S4. Similarly, starting with the symmetrical equal-alternative case prior to the stop-signal bifurcation (Fig. S3A, the initial, symmetrically located stable fixed-point moves towards the part of the phase plane corresponding to the superior alternative, and the system will then also be expected to converge on choosing that superior alternative.

The discriminate stop-signal decision-making process is therefore able to adapt according to the choice at hand: if the alternatives are equal it will, with sufficient stop signaling, avoid deadlock by randomly but decisively choosing either alternative quickly; but if the alternatives are sufficiently unequal, it will always be expected to converge on correctly choosing the superior alternative, regardless of the extent of stop signaling.

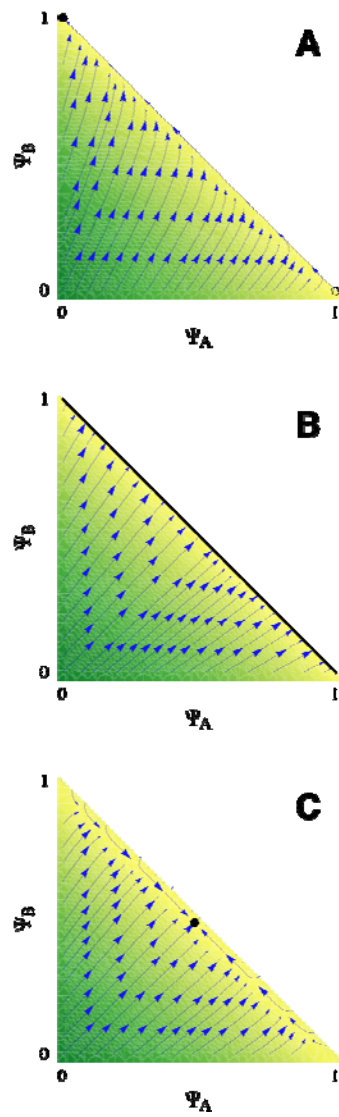


Fig. S1.

Dynamical behavior of the process of decision making by direct switching. The stable/unstable fixed-points are shown as filled/open black circles. The stable manifold is

shown as a thick black line. **(A)** Asymptotically optimal case for unequal alternatives: $\gamma_A = 3, \gamma_B = 6, \alpha_A = 0, \alpha_B = 0, \rho_A = 3, \rho_B = 6, \delta_A = 1, \delta_B = 2$. **(B)** Asymptotically optimal case for equal alternatives: $\gamma = 3, \alpha = 0, \rho = 3, \delta = 1$. **(C)** General case with finite decay for equal alternatives: $\gamma = 3, \alpha = 1/3, \rho = 3, \delta = 1$.

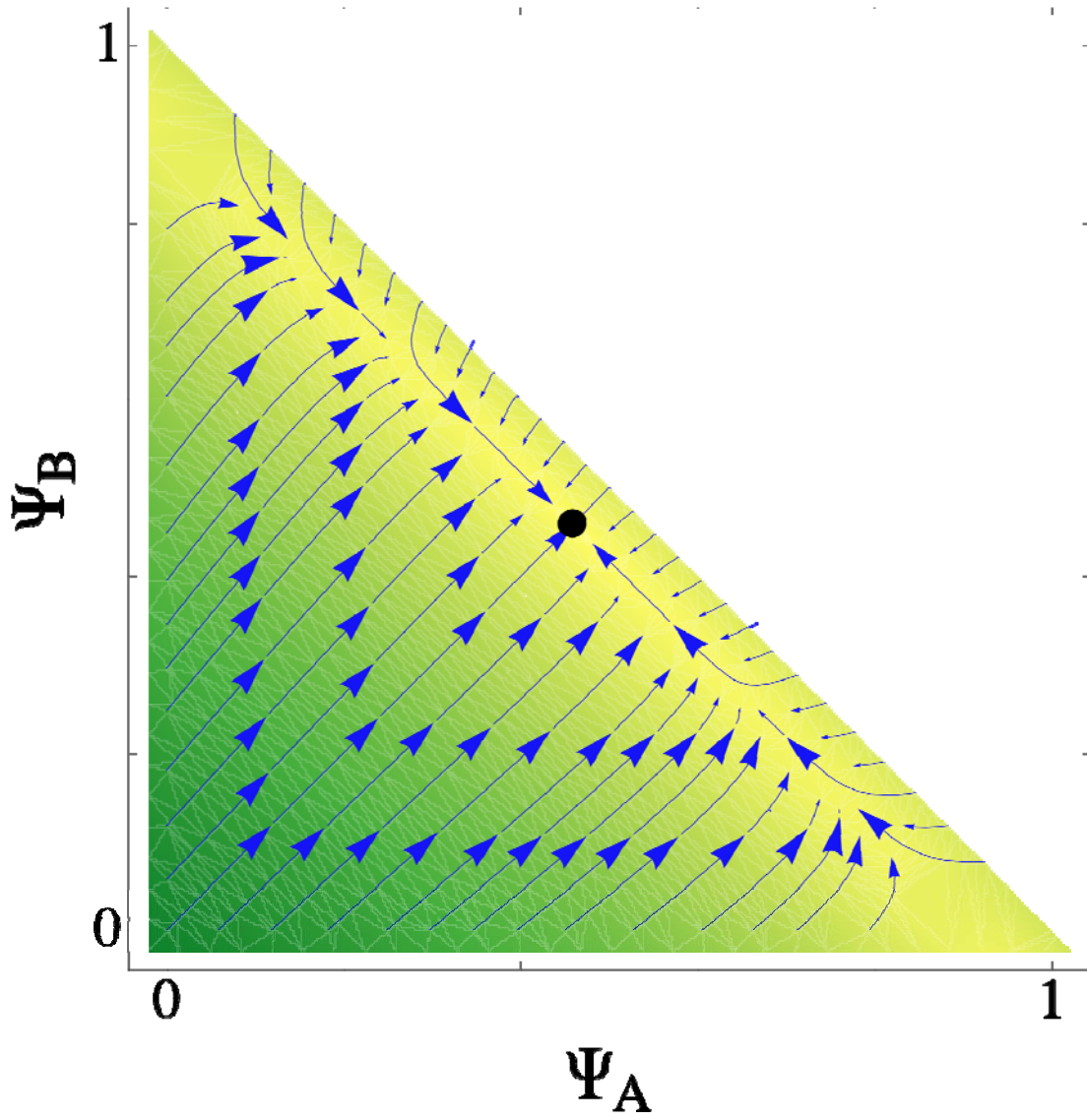


Fig. S2

Dynamical behavior of the process of decision making with indiscriminate stop signal for the case of equal alternatives: $\gamma = 3$, $\alpha = 1/3$, $\rho = 3$, $\sigma = 1$. The stable fixed-point is shown as a filled black circle.

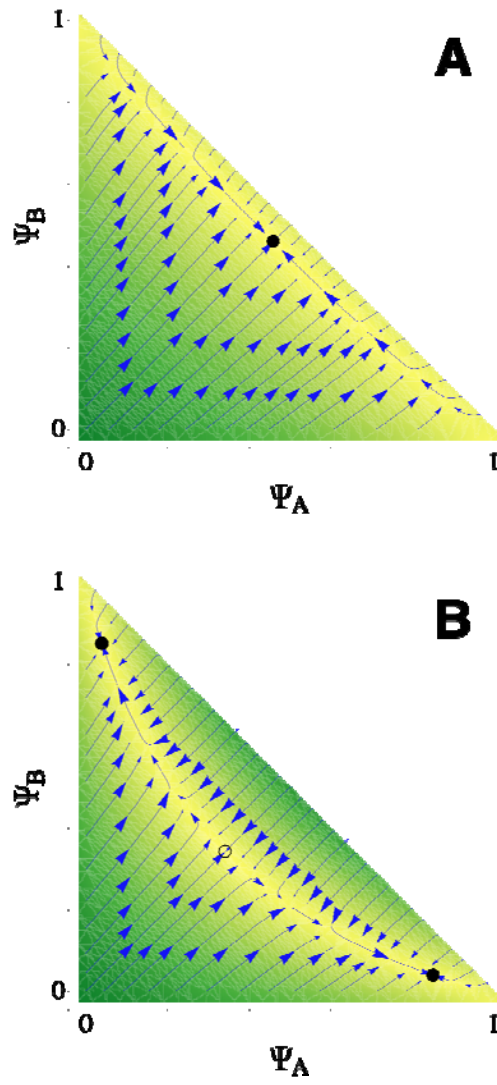


Fig. S3

Dynamical behavior of the process of decision making with discriminate stop signal for the case of equal alternatives. The stable/unstable fixed-points are shown as filled/open

black circles. **(A)** Prior to the stop-signal bifurcation: $\gamma = 3$, $\alpha = 1/3$, $\rho = 3$, $\sigma = 1$. **(B)** After the stop-signal bifurcation: $\gamma = 3$, $\alpha = 1/3$, $\rho = 3$, $\sigma = 10$.

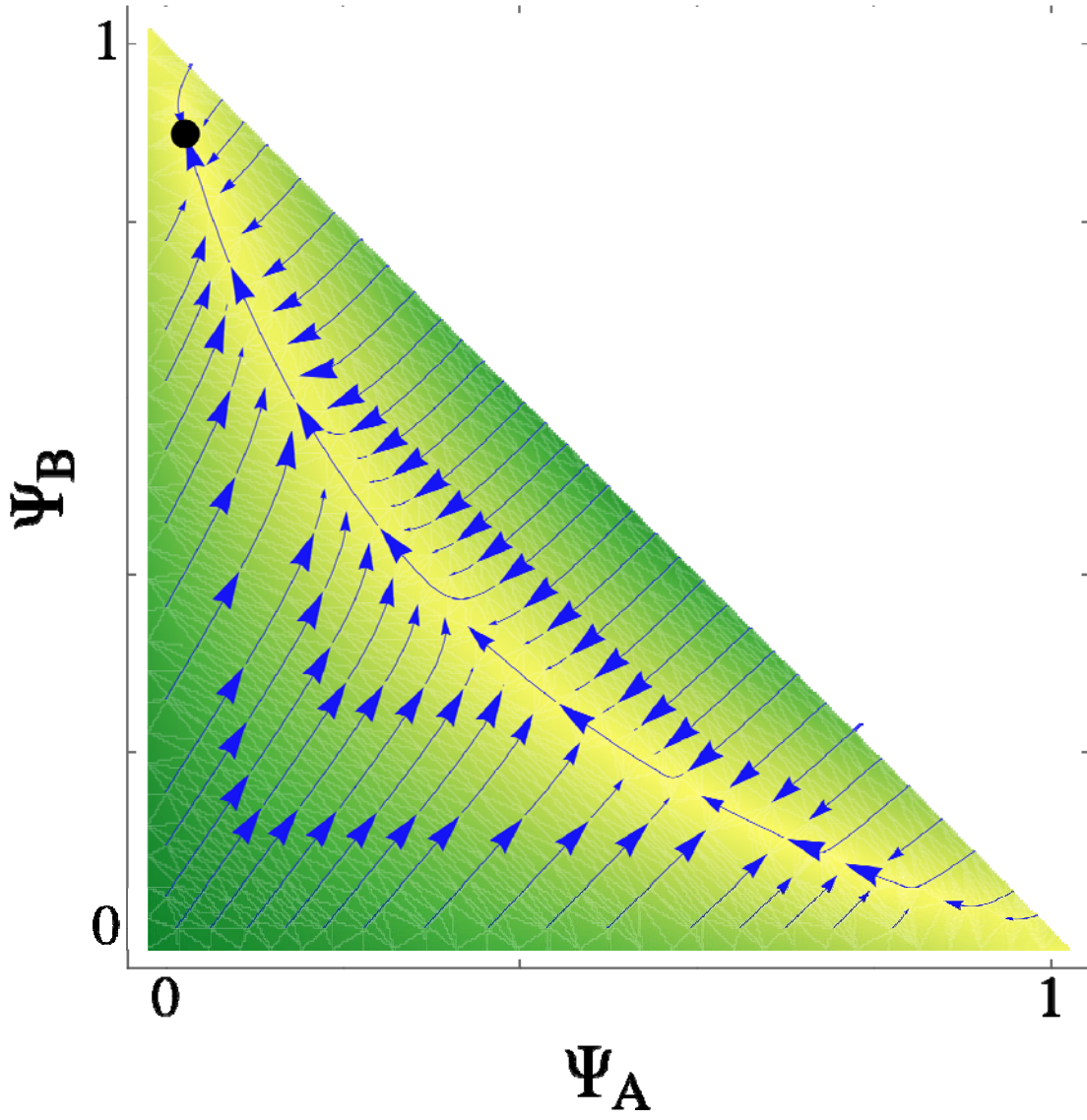


Fig. S4.

Dynamical behavior of the process of decision making with discriminate stop signal for the case of unequal alternatives: $\langle \gamma \rangle = 3$, $\Delta \gamma = -1$, $\langle \alpha \rangle = 1/3$, $\Delta \alpha = 0$, $\langle \rho \rangle = 3$, $\Delta \rho = 0$, $\langle \sigma \rangle = 10$, $\Delta \sigma = 0$. The stable fixed-point is shown as a filled black circle.

Table S1.

Data on stop signals received by 40 scouts performing waggle dances on 2 swarms.

Swarm	Dancer	Dance duration (sec)	Dance circuits	Number of stop signals received	Stop Signal					
					Stop signal number	Stop signaler	Signal duration (frames)	Circuits followed before signaling	Phase	
SWARM 1	1	1	220	63	2	1	first	8	2	waggle
						2	second	5		return
	1	2	43	7	1	1	first	5	1	return
	1	3	125	30	1	1	first	3	3	return
	1	4	27	5	0					
	1	5	74	25	0					
	1	6	13	4	2	1	first	5	2	return
	1					2	first	5		return
	1	7	42	13	0					
	1	8	50	16	5	1	first	17	4	return
						2	first	2		waggle
						3	first	4		return
						4	first	4		return
						5	first	3		return
	1	9	31	9	0					
	1	10	47	26	3	1	first	4	2	return
						2	first	4		return
						3	second	15	3	return
	1	11	28	6	1	1	first	6	3	return
	1	12	266	86	7	1	first	4	3	return
						2	first	3		return
						3	second	6	1	return
						4	second	5		return
						5	second	7		return
						6	third	8	3	return
						7	third	7		return
	1	13	59	18	8	1	first	8	1	return
						2	second	9	3	return
						3	second	5		return
						4	third	6	2	return
						5	third	5		return
						6	third	5		return
						7	third	4		waggle
						8	fourth	5	5	waggle
	1	14	67	26	9	1	first	4	3	return
						2	first	7		return
					3	second	4	3	return	
					4	third	5	3	return	

SWARM 2						5	third	5		return
						6	third	8		waggle
						7	third	6		return
						8	third	5		return
						9	third	6		return
	1	15	28	3	0					
	1	16	57	12	0					
	1	17	62	13	3	1	first	4	2	return
						2	first	5		return
						3	second	3	2	return
	1	18	37	4	1	1	first	5	2	return
	1	19	38	9	11	1	first	4		waggle
						2	first	4		return
						3	first	4		return
						4	second	8	2	return
						5	second	4		return
						6	second	3		return
						7	third	4	4	return
						8	third	4		return
						9	third	4		return
						10	third	4		waggle
						11	third	6		return
	1	20	35	6	0					
	2	1	52	14	2	1	first	5	1	return
						2	first	4		waggle
	2	2	111	36	0					
	2	3	48	17	0					
	2	4	48	20	0					
	2	5	58	22	1	1	first	6	9	return
	2	6	19	3	1	1	first	7	2	return
	2	7	145	50	2	1	first	7	6	return
						2	first	6		return
	2	8	110	42	0					
	2	9	128	34	0					
	2	10	82	19	0					
	2	11	71	20	1	1	first	4	3	return
	2	12	82	28	10	1	first	10	3	return
						2	second	6	2	return
						3	second	7		return
						4	second	8		return
						5	second	6		return
						6	third	6	2	return
						7	fourth	6	4	return
						8	fourth	5		return
						9	fifth	7	3	return
						10	fifth	6		return
	2	13	39	12	11	1	first	8	2	return

					2	first	8		return
					3	first	6		return
					4	first	10		return
					5	first	9		return
					6	first	8		return
					7	first	5		return
					8	first	8		return
					9	first	7		return
					10	first	10		return
					11	first	7		return
2	14	107	48	0					
2	15	21	3	2	1	first	6	2	waggle
					2	first	7		waggle
2	16	142	67	0					
2	17	39	9	0					
2	18	76	31	15	1	first	20	3	return
					2	second	12	2	return
					3	first	10	2	return
					4	second	5	3	return
					5	second	6		return
					6	first	12	4	return
					7	second	12	3	return
					8	third	18	4	waggle
					9	third	12		return
					10	second	8	5	return
					11	fourth	12	3	return
					12	fourth	9		return
					13	fifth	5	4	waggle
					14	sixth	13	6	return
2	19	96	38	10	15	fifth	6	2	return
					1	first	6	3	return
					2	first	6		return
					3	second	6	2	return
					4	second	6		return
					5	third	6	6	return
					6	third	5		return
					7	third	6		waggle
					8	third	7		return
					9	third	5		return
2	20	147	54	0	10	third	5		return

Distribution of stop signals (“beeps”) across dances for three swarms. Numbers indicate the dance circuits during which a dancer received stop signals.

		Total # of dance circuits	Number of stop signals	Beep #1	Beep #2	Beep #3	Beep #4	Beep #5	Beep #6	Beep #7	Beep #8	Beep #9	Beep #10	Beep #11	Beep #12	Beep #13	Beep #14	Beep #15	Beep #16	Beep #17	Beep #18	Beep #19
Swarm	Dance																					
1	1	123	6	11	15	68	69	81	83													
1	2	8	4	1	5	6	8															
1	3	3	3	2	2	3																
1	4	141	1	90																		
1	5	13	7	12	13	13	13	13	13	13												
1	6	60	1	37																		
1	7	57	2	12	37																	
1	8	2	1	2																		
1	9	71	11	6	34	37	57	58	61	67	68	69	70	71								
1	10	1	1	1																		
1	11	54	2	6	13																	
1	12	51	1	50																		
1	13	42	4	36	39	40	42															
1	14	12	2	11	12																	
1	15	22	5	8	8	14	15	21														
1	16	13	1	2																		
1	17	9	1	7																		
1	18	25	3	15	16	17																
1	19	6	2	5	6																	
1	20	65	3	3	4	12																
1	21	18	1	13																		
1	22	16	3	10	10	11																
1	23	17	2	14	16																	
1	24	8	3	3	4	4																
1	25	6	2	6	6																	
1	26	38	1	19																		
1	27	47	1	26																		
1	28	35	1	12																		
1	29	37	1	5																		
1	30	47	2	45	46																	
1	31	12	2	4	5																	
1	32	11	1	8																		
1	33	20	1	17																		
1	34	49	4	18	41	44	46															
1	35	15	1	8																		
1	36	13	2	6	11																	
1	37	64	1	5																		
1	38	46	2	41	43																	
1	39	32	7	1	1	2	11	11	13	14												
1	40	8	2	4	6																	
1	41	6	9	1	2	4	5	5	6	6	6	6										
1	42	10	2	7	8																	
1	43	71	8	5	6	7	8	8	9	10	18	33	71									
1	44	23	1	4																		
1	45	14	2	11	12																	
1	46	21	1	7																		
1	47	44	5	20	35	38	41	42														
1	48	75	5	17	42	59	74	75														
1	49	76	5	1	3	4	5	17														
1	50	30	10	6	27	27	27	28	28	28	29	29	30	30								
1	51	38	12	2	2	3	4	4	5	5	6	6	7	7	34							
1	52	162	3	13	114	115																
1	53	32	2	25	27																	

[illegible]

Movie S1

In this video clip, you see a dancing scout bee from nest site A (with blue and yellow paint marks on her thorax) receive three stop signals from a scout bee from nest site B (with a pink paint mark on her thorax). Notice how each time the “pink” scout bee produces a stop signal, she vigorously butts her head against the “blue-yellow” scout bee. The object in the lower left corner of the image is the microphone that recorded the brief, high-pitched beep sounds of the stop signals.

References and Notes

1. K. M. Passino, T. D. Seeley, P.K. Visscher, Swarm cognition in honey bees, *Behav. Ecol. Sociobiol.* **62**, 401 (2008).
2. I. D. Couzin, Collective cognition in animal groups, *Trends Cogn. Sci.* **13**, 36 (2008).
3. J. A. R. Marshall, R. Bogacz, A. Dornhaus, R. Planqué, T. Kovacs, N. R. Franks, On optimal decision-making in brains and social insect colonies, *J. R. Soc. Interface* **6**, 1065 (2009).
4. S. C. Pratt, E. B. Mallon, D. J. T. Sumpter, N. R. Franks, Quorum sensing, recruitment, and collective decision-making during colony emigration by the ant *Leptothorax albigipennis*, *Behav. Ecol. Sociobiol.* **52**, 117 (2005).
5. P. W. Glimcher, The neurobiology of visual-saccadic decision making, *Annu. Rev. Neurosci.* **26**, 133 (2003).
6. T.D. Seeley, P.K. Visscher, Quorum sensing during nest-site selection by honeybee swarms, *Behav. Ecol. Sociobiol.* **56**, 594 (2004).
7. J. I. Gold, M. N. Shadlen, The neural basis of decision making, *Annu. Rev. Neurosci.* **30**, 535 (2007).
8. M. Usher, J. L. McClelland, The time course of perceptual choice: the leaky, competing accumulator model, *Psychol. Rev.* **108**, 550 (2001).
9. X. J. Wang, Probabilistic decision making by slow reverberation in cortical circuits, *Neuron* **36**, 955 (2002).
10. R. Bogacz, E. Brown, J. Moehlis, P. Holmes, J. D. Cohen, The physics of optimal decision making: a formal analysis of models of performance in two-alternative forced-choice tasks, *Psychol. Rev.* **113**, 700 (2006).
11. T. D. Seeley, P. K. Visscher, K. M. Passino, Group decision making in honey bee swarms, *Amer. Sci.* **94**, 220 (2006).
12. T. D. Seeley, *Honeybee Democracy* (Princeton Univ. Press, Princeton, NJ, 2010).
13. J. C. Nieh, The stop signal of honey bees: reconsidering its message, *Behav. Ecol. Sociobiol.* **33**, 51 (1993).

14. W. H. Kirchner, Vibrational signals in the tremble dance of the honeybee, *Apis mellifera*, *Behav. Ecol. Sociobiol.* **33**, 169 (1993).
15. K. A. Pastor, T.D. Seeley, The brief piping signal of the honey bee: begging call or stop signal? *Ethology* **111**, 775 (2005).
16. J. C. Nieh, A negative feedback signal that is triggered by peril curbs honey bee recruitment, *Curr. Biol.* **20**, 310 (2010).
17. A. Michelsen, W. H. Kirchner, M. Lindauer, Sounds and vibrational signals in the dance language of the honeybee, *Apis mellifera*, *Behav. Ecol. Sociobiol.* **18**, 207 (1986).
18. Materials and methods are available as supporting material on *Science* Online.
19. T. D. Seeley, J. Tautz, Worker piping in honey bee swarms and its role in preparing for liftoff, *J. Comp. Physiol. A* **187**, 667 (2001).
20. T. D. Seeley, P. K. Visscher, Choosing a home: how the scouts in a honey bee swarm perceive the completion of their group decision making, *Behav. Ecol. Sociobiol.* **54**, 511 (2003).
21. M. Lindauer, Schwarmbienen auf Wohnungssuche, *Z. vergl. Physiol.* **37**, 263 (1955).
22. T. D. Seeley, Consensus building during nest-site selection in honey bee swarms: the expiration of dissent, *Behav. Ecol. Sociobiol.* **53**, 417 (2003).
23. T. D. Seeley, P. K. Visscher, Sensory coding of nest-site value in honeybee swarms, *J. Exp. Biol.* **211**, 3691 (2008).
24. R. Bogacz, Optimal decision-making theories: linking neurobiology with behaviour, *Trends Cogn. Sci.* **11**, 118 (2007).
25. G. F. Combs, Jr. The engorgement of swarming worker honeybees, *J. Apic. Res.* **11**, 121 (1972).
26. M. A. Leta, C. Gilbert, R. A. Morse, Levels of hemolymph sugars and body glycogen of honeybees (*Apis mellifera* L.) from colonies preparing to swarm, *J. Insect Physiol.* **42**, 239 (1996).
27. T. D. Seeley, S. C. Buhrman, Group decision making in swarms of honey bees, *Behav. Ecol. Sociobiol.* **45**, 19 (1999).
28. M. Beekman, R. L. Fathke, T. D. Seeley, How does an informed minority of scouts guide a honey bee swarm as it flies to its new home? *Anim. Behav.* **71**, 161 (2006).
29. C. Mitchell, Weights of workers and drones, *Am. Bee J.* **110**, 468 (1970).
30. T. D. Seeley, S. C. Buhrman, Nest-site selection in honey bees: how well do swarms implement the “best-of-N” decision rule? *Behav. Ecol. Sociobiol.* **49**, 416 (2001).
31. P. K. Visscher, T. D. Seeley, Coordinating a group departure: who produces the piping signals on honeybee swarms? *Behav. Ecol. Sociobiol.* **61**, 1615 (2007).
32. R. Ratcliffe, A theory of memory retrieval, *Psychol. Rev.* **85**, 59 (1978).

33. J. Ditterich, Stochastic models of decisions about motion direction: behavior and physiology. *Neural Networks* **19**, 981 (2006).
34. M. S. de La Lama, I. G. Szendro, J. R. Iglesias, H. S. Wio, Van Kampen's expansion approach in an opinion formation model. *Eur. Phys. J. B* **51**, 435 (2006).
35. T. Galla, Independence and interdependence in the nest-site choice by honeybee swarms: Agent-based models, analytical approaches and pattern formation, *J. Theor. Biol.* **262**, 186 (2010).
36. N. Stroeymeyt, E. J. H. Robinson, P. M. Hogan, J. A. R. Marshall, M. Giurfa, N. R. Franks, Experience-dependent flexibility in collective decision making by house-hunting ants, *Behav. Ecol.* **22**, 535 (2011).
37. K. H. Britten, M. N. Shadlen, W. T. Newsome, J. A. Moshon, Responses of neurons in macaque MT neurons to stochastic motion signals, *Vis. Neurosci.* **10**, 1157 (1993).
38. A. C. Huk, M. N. Shadlen, Neural activity in macaque parietal cortex reflects temporal integration of visual motion signals during perceptual decision making, *J. Neurosci.* **25**, 10420 (2005).
39. T. D. Hanks, J. Ditterich, M. N. Shadlen, Microstimulation of macaque area LIP affects decision-making in a motion discrimination task, *Nature Neurosci.* **9**, 682 (2006).
40. N. G. van Kampen, *Stochastic Processes in Physics and Chemistry*, 3rd ed., (North-Holland, Amsterdam, 2007).
41. J. D. Schall, Neural basis of deciding, choosing and acting. *Nature Rev. Neurosci.* **2**, 33 (2001).
42. M. N. Shadlen, W. T. Newsome, Neural basis of a perceptual decision in the parietal cortex (area LIP) of the rhesus monkey, *J. Neurophysiol.* **86**, 1916 (2001).
43. J. D. Roitman, M. N. Shadlen, Response of neurons in the lateral intraparietal area during a combined visual discrimination reaction time task. *J. Neurosci.* **22**, 9475 (2002).
44. F. Hayot, C. Jayaprakash, The linear noise approximation for molecular fluctuations within cells, *Phys. Biol.* **1**, 205 (2004).